

Charged particle rapidity distributions at RHIC

Zi-wei Lin¹, Subrata Pal¹, C.M. Ko¹, Bao-An Li², and Bin Zhang²

¹*Cyclotron Institute and Physics Department, Texas A&M University, College Station, Texas 77843-3366*

²*Department of Chemistry and Physics, Arkansas State University, P.O. Box 419, State University, Arkansas 72467-0419*

Using a multiphase transport model (AMPT), which includes both initial partonic and final hadronic interactions, we study the rapidity distributions of charged particles such as protons, antiprotons, pions, and kaons in heavy ion collisions at RHIC. The theoretical results for the total charged particle multiplicity at midrapidity are consistent with those measured by the PHOBOS collaboration in central Au+Au collisions at $\sqrt{s} = 56$ and 130 AGeV. We find that these hadronic observables are much more sensitive to the hadronic interactions than the partonic interactions.

PACS numbers: 25.75.-q, 24.10.Lx

Collisions of nuclei at high energies offer the possibility to subject nuclear matter to the extreme conditions of large compression and high excitation energies. Studies based on both non-equilibrium transport models [1] and equilibrium thermal models [2] have shown that the experimental data from heavy ion collisions at SIS, AGS and SPS, where the center of mass collision energies are, respectively, about 3, 5 and 17 AGeV, are consistent with the formation of a hot dense nuclear matter in the initial stage of collisions. With the Relativistic Heavy Ion Collider (RHIC) at Brookhaven National Laboratory, which can reach a center of mass energy of 200 AGeV, the initial energy density is expected to exceed that for the transition from the hadronic matter to the quark-gluon plasma. Experiments at RHIC thus provide the opportunity to recreate the matter which is believed to have existed during the first microsecond after the Big Bang and to study its properties.

Recently, charged particle multiplicity near mid-rapidity has been measured in central Au+Au collisions at $\sqrt{s} = 56$ and 130 AGeV at RHIC by the PHOBOS collaboration [3]. The observed charged particle density per participant is found to be compatible with the predictions of the HIJING model that includes particle production from minijets produced in hard-scattering processes [4]. Although the HIJING model implements the parton energy loss via jet quenching [5], it does not include explicit interactions among minijet partons and the final-state interactions among hadrons. Other models have also been used to understand the data from the PHOBOS collaboration. The LEXUS model [6], which is based on a linear extrapolation of ultra-relativistic nucleon-nucleon scattering to nucleus-nucleus collisions, predicts too many charged particles compared with the PHOBOS data [7]. On the other hand, the hadronic cascade model LUCIFER [8] predicts a charged particle multiplicity near mid-rapidity that is comparable to the PHOBOS data [9]. In this paper, we shall use a recently developed multiphase transport model (AMPT) [10], that includes both partonic and hadronic interactions, to study their effects not only on the total charged particle multiplicity but also on those of kaons, protons, and antiprotons.

In the AMPT model, the initial conditions are obtained from the HIJING model [4] by using a Woods-Saxon radial shape for the colliding nuclei and including the nuclear shadowing effect on parton production via the gluon recombination mechanism of Mueller-Qiu [11]. After the colliding nuclei pass through each other, the Gyulassy-Wang model [12] is then used to generate the initial space-time information of partons. In the default HIJING, these minijet partons are allowed to lose energy via the gluon splitting mechanism and transfer their energies to the nearby strings associated with initial soft interactions. Such jet quenching is replaced in the AMPT model by explicitly taking into account parton-parton collisions via Zhang's Parton Cascade (ZPC) [13]. At present, only gluon elastic scatterings are included, so the partons do not suffer any inelastic energy loss as they traverse the dense matter. After partons stop interacting, they combine with their parent strings and are then converted to hadrons using the Lund string fragmentation model [14,15] after an average proper formation time of 0.7 fm/c. Dynamics of the resulting hadronic matter is described by a relativistic transport model (ART) [16], which has been improved to include baryon-antibaryon production from meson-meson interactions and their annihilation using cross sections given in Ref. [17,18]. Also, the K^* resonances are explicitly treated by including their production from pion-kaon and pion-rho scatterings [19] and the inverse reactions of decay and absorption.

We first determine the parameters in the AMPT model by fitting the experimental data from central Pb+Pb collisions at center of mass energy of 17 AGeV [20]. Specifically, to describe the measured net baryon rapidity distribution, we have included in the Lund string fragmentation model the popcorn mechanism for baryon-antibaryon production with equal probabilities for baryon-meson-antibaryon and baryon-antibaryon configurations [10]. Also, to account for pion and the enhanced kaon yields in the preliminary data from the same reaction, we have modified two other parameters in the Lund string fragmentation model, following the expectation that the string tension is increased in the dense matter formed in the initial stage of heavy ion collisions.

In the Lund string fragmentation model as implemented in the JETSET/PYTHIA routine [15], one first assumes that a string fragments into quark-antiquark pairs with a Gaussian distribution in transverse momentum. Also, a suppression factor of 0.30 is used for strange quark-antiquark pair production relative to the light quark-antiquark pair production. Hadrons are then formed from these quarks and antiquarks. For a hadron with a given transverse momentum m_{\perp} determined by those of its quarks, its longitudinal momentum is given by the splitting function [14,15],

$$f(z) \propto z^{-1}(1-z)^a \exp(-b m_{\perp}^2/z), \quad (1)$$

where z is the light-cone momentum fraction of the produced hadron with respect to that of the fragmenting string. Based on the Schwinger mechanism for particle production in a strong field, the production probability is proportional to $\exp(-\pi m_{\perp}^2/\kappa)$, where κ is the string tension, i.e., energy in a unit length of string. The average squared transverse momentum of produced particle is thus proportional to κ . Increasing the string tension then leads to a broader distribution of the transverse momenta of produced quark-antiquark pairs and also a reduced suppression for strange quark-antiquark pairs. Since the average squared transverse momenta of produced particles obtained from Eq. (1) is $\langle p_{\perp}^2 \rangle = [b(2+a)]^{-1}$ for massless particles, the two parameters a and b are approximately related to the string tension by $\kappa \propto [b(2+a)]^{-1}$. In the HIJING model, the default values for a and b are 0.5 and 0.9 GeV^{-2} , respectively. We change their values to 2.2 and 0.5 GeV^{-2} in order to increase, respectively, the pion and kaon multiplicities. These values of a and b correspond to a 7% increase of the string tension.

Results from the AMPT model for Pb+Pb collisions at $\sqrt{s} = 17$ AGeV, based on the above modification of the HIJING and ART models, are shown in Fig. 1. It is seen that our model gives a reasonable description of the data on the rapidity distributions of total and negatively charged particles, net-protons and antiprotons, charged pions, and charged kaons. Since the probability for mini-jet production is very small in collisions at SPS energies, the partonic stage does not play any role in the collisions. We find that final-state hadronic scatterings reduce the production of kaons and antikaons by about 20%. In contrast, kaon yields in the default HIJING model are smaller than our final results by about 40%.

Since the number of strings associated with soft interactions in the HIJING model depends weakly on the colliding energy, the parameters in the string fragmentation model are not expected to change much with the energy. We thus use the same parameters determined from the experimental data at SPS to study heavy ion collisions at RHIC energies. In Fig. 2, the results for central Au+Au collisions at center of mass energies of 56 AGeV (dashed curves) and 130 AGeV (solid curves) are shown together with the data from the PHOBOS collaboration

[3]. The measured total charged particle multiplicities at mid-pseudorapidity at both energies are well reproduced by our model.

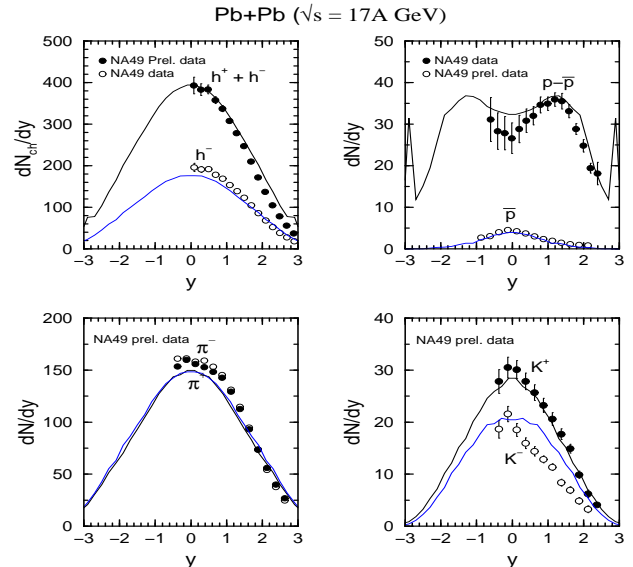


FIG. 1. Rapidity distributions of total and negatively charged particles (upper left panel), net-protons and antiprotons (upper right panel), charged pions (lower left panel), and charged kaons (lower right panel) in heavy ion collisions at $\sqrt{s} = 17$ AGeV. The circles are the experimental data for 5% most central Pb+Pb collision from the NA49 Collaboration, and the solid curves are the AMPT model calculations for impact parameters of $b \leq 3$ fm.

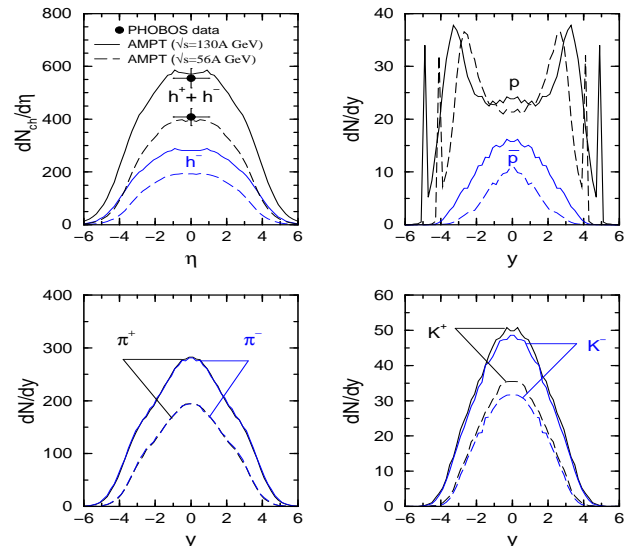


FIG. 2. Same as Fig. 1 but for Au+Au collisions at $\sqrt{s} = 56$ and 130 AGeV. The solid circles are the PHOBOS data for 6% most central collisions while the curves are the AMPT calculations for $b \leq 3$ fm.

The energy dependence of charged particle yields at mid-rapidity from the SPS to RHIC energies is shown in Fig. 3. The proton yield is seen to have a minimum at energies between SPS and the highest energy at RHIC, while antiproton yield increases almost linearly with $\ln s$. As a result, the \bar{p}/p ratio increases rapidly from about 0.1 at SPS to about 0.8 at the RHIC energy of $\sqrt{s} = 200$ AGeV, indicating the formation of a nearly baryon-antibaryon symmetric matter at high energies. Meson yields in general exhibit a faster increase with energy; in particular, we find that the K^+/π^+ ratio is almost constant within this energy range, suggesting the approximate chemical equilibrium for strangeness production. The K^-/K^+ ratio increases gradually from 0.7 at SPS to about 1.0 at $\sqrt{s} = 200$ AGeV as a result of the nearly baryon-antibaryon symmetric matter formed at high energies.

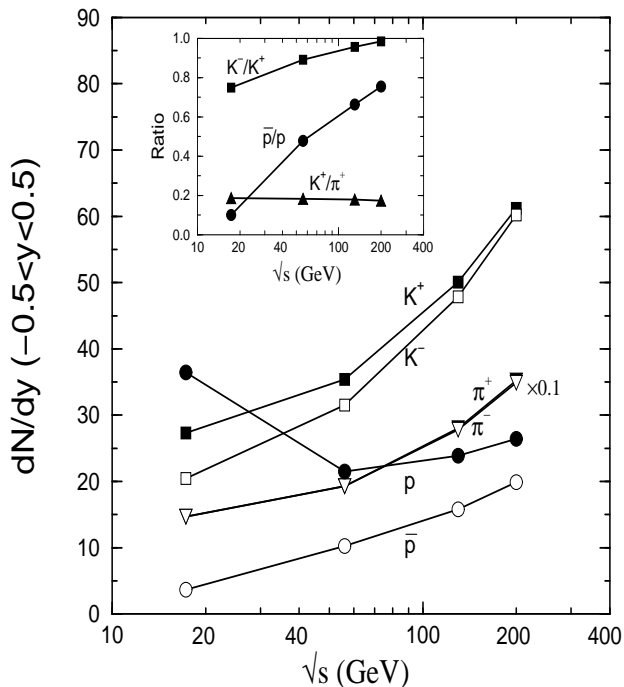


FIG. 3. Energy dependence of charged particle yields at mid-rapidity. The ratios of K^-/K^+ , \bar{p}/p and K^+/π^+ are shown in the insert.

To see the effects of hadronic interactions, we show in Fig. 4 by dashed curves the rapidity distributions of charged particles obtained from the AMPT model without the ART model for central Au+Au collisions at 130 AGeV. In this case, there is a significant increase in the numbers of total charged particles, pions, protons, and antiprotons at midrapidity. The kaon number is, on the

other hand, reduced slightly. As a result, the ratios of \bar{p}/p and K^+/π^+ in the absence of final-state hadronic interactions are 0.80 and 0.13, respectively, instead of 0.66 and 0.18 from the default AMPT model. We note that although the default HIJING [5] gives a total charged particle multiplicity at midrapidity that is consistent with the PHOBOS data, including hadronic scatterings would reduce its prediction appreciably.

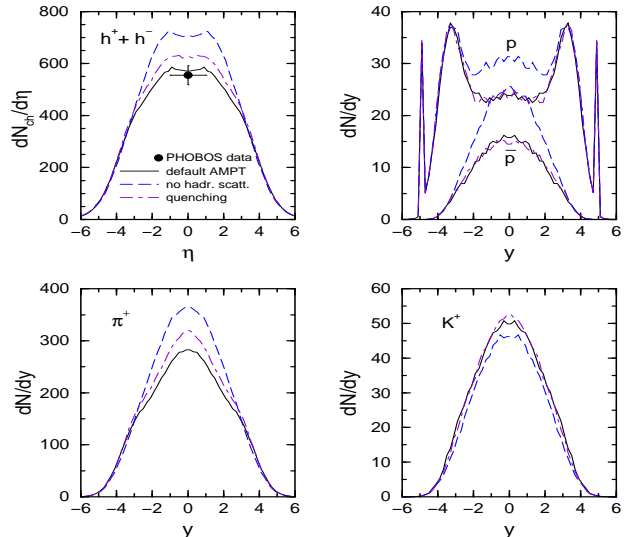


FIG. 4. Rapidity distributions of charged particles for central ($b \leq 3$ fm) Au+Au collisions at 130 AGeV from AMPT model with default parameters (solid curves), without hadronic scatterings (dashed curves), and with jet quenching of $dE/dx = 1$ GeV/fm (dot-dashed curves).

Effects of partonic dynamics on the final hadronic observables can also be studied in the AMPT model. Turning off the partonic cascade in the AMPT model, we find that this leads to less than $\sim 5\%$ change in the final charged particle yields at $\sqrt{s} = 130$ AGeV. This indicates that the multiplicity distribution of hadrons are not very sensitive to parton elastic scatterings. To take into account the effect of parton inelastic collisions, which are mostly responsible for energy loss, we include in the AMPT model also the default jet quenching, i.e., an energy loss of $dE/dx = 1$ GeV/fm, before minijet partons enter the ZPC parton cascade. The results with jet quenching for central Au+Au collisions at 130 AGeV are shown in Fig. 4 by the dot-dashed curves. We see that the quenching effects are larger for pions than for kaons, protons, and antiprotons. Since the present calculations from the AMPT model without jet quenching already reproduce the data at the energy of 130 AGeV, and further inclusion of jet quenching of $dE/dx = 1$ GeV/fm entails a 10% increase of the final yield of total charged particles at midrapidity, our results for the rapidity distribution of charged particles are thus consistent with none or a weak jet quenching at this energy.

We note that without initial nuclear shadowing on parton production the charged particle multiplicity at mid-rapidity at 130 AGeV increases by about 30%. This increase can nevertheless be offset by using different values for the parameters in the Lund string fragmentation. Since nuclear shadowing has negligible effects at SPS energies due to insignificant production of minijets, to reproduce both SPS and RHIC data using the same parameters requires the inclusion of nuclear shadowing on parton production.

In summary, using a multiphase transport model (AMPT), which includes both initial partonic and final hadronic interactions, we have studied the rapidity distributions of charged particles such as protons, antiprotons, pions, and kaons in heavy ion collisions at RHIC. With the model parameters constrained by central Pb+Pb collisions at $\sqrt{s} = 17$ AGeV at SPS, the theoretical results on the total charged particle multiplicity at midrapidity in central Au+Au collisions at $\sqrt{s} = 56$ and 130 AGeV agree quite well with the data from the PHOBOS collaboration. We find that the antiproton to proton ratio at mid-rapidity increases appreciably with \sqrt{s} , indicating the approach to a near baryon-antibaryon symmetric matter in high energy collisions. Furthermore, the K^+/π^+ ratio is almost constant within the energy range studied here, suggesting the approximate chemical equilibrium for strangeness production in these collisions. These hadronic observables are, however, less sensitive to the initial partonic interactions than the final hadronic interactions. To observe the effects of the partonic matter formed in the initial stage thus requires measurements of other observables such as J/ψ suppression [21], the elliptic flow [22], and high p_\perp spectra [23]. The magnitude of elliptic flow has been shown to be sensitive to the parton-parton cross sections in the ZPC parton cascade model [24], and the J/ψ suppression results using the AMPT model indicate that the partonic matter plays a much stronger role than the hadronic matter [25].

The work of Z.L., S.P. and C.M.K. was supported by the National Science Foundation under Grant No. PHY-9870038, the Welch Foundation under Grant No. A-1358, and the Texas Advanced Research Program under Grant No. FY99-010366-0081, while that of B.A.L. was supported by the National Science Foundation under Grant No. PHY-0088934 and Arkansas Science and Technology Authority Grant No. 00-B-14.

- [1] C.M. Ko and G.Q. Li, J. Phys. G **22**, 1673 (1996); S. Bass *et al.*, Prog. Part. Nucl. Phys. **41**, 225 (1998); W. Cassing and E. Bratkovskaya, Phys. Rep. **308**, 65 (1999).
- [2] P. Braun-Munzinger, J. Stachel, J.P. Wessel, and N. Xu, Phys. Lett. B **344**, 43 (1995); B **365**, 1 (1996); P. Braun-Munzinger, I. Heppe, and J. Stachel, Phys. Lett. B **465**, 15 (1999).
- [3] B.B. Back *et al.* (PHOBOS Collaboration), Phys. Rev. Lett. **85**, 3100 (2000).
- [4] X.N. Wang and M. Gyulassy, Phys. Rev. D **44**, 3501 (1991); M. Gyulassy and X.N. Wang, Comp. Phys. Comm. **83**, 307 (1994).
- [5] X.N. Wang and M. Gyulassy, Phys. Rev. Lett. **86**, 3496 (2001).
- [6] S. Jeon and J. Kapusta, Phys. Rev. C **56**, 468 (1997).
- [7] S. Jeon and J. Kapusta, Phys. Rev. C **63**, 011901 (2001).
- [8] D.E. Kahana and S.H. Kahana, Phys. Rev. C **58**, 3574 (1998); C **59**, 1651 (1999).
- [9] D.E. Kahana and S.H. Kahana, Phys. Rev. C **63**, 031901 (2001).
- [10] B. Zhang, C.M. Ko, B.A. Li, and Z. Lin, Phys. Rev. C **61**, 067901 (2000).
- [11] A.H. Mueller and J. Qiu, Nucl. Phys. B **268**, 427 (1986); J. Qiu, Nucl. Phys. B **291**, 746 (1987).
- [12] M. Gyulassy and X.N. Wang, Nucl. Phys. B **420**, 583 (1994).
- [13] M. Gyulassy, Y. Pang, and B. Zhang, Nucl. Phys. A **626**, 999 (1997); B. Zhang, Comp. Phys. Comm. **109**, 193 (1998).
- [14] B. Andersson, G. Gustafson, G. Ingelman, and T. Sjöstrand, Phys. Rep. **97**, 31 (1983); B. Andersson, G. Gustafson, and B. Soderberg, Z. Phys. C **20**, 317 (1983).
- [15] T. Sjöstrand, Comp. Phys. Comm. **82**, 74 (1994). Program updates and documentation can be found at <http://www.thep.lu.se/tf2/staff/torbjorn/Pythia.html>.
- [16] B.A. Li and C.M. Ko, Phys. Rev. C **52**, 2037 (1995).
- [17] G.J. Wang, G. Welke, R. Bellwied, and C. Pruneau, nucl-th/9807036.
- [18] C.M. Ko and R. Yuan, Phys. Lett. B **192**, 31 (1987).
- [19] G.E. Brown, C.M. Ko, Z.G. Wu, and L.H. Xia, Phys. Rev. C **43**, 1881 (1991).
- [20] H. Appelshäuser *et al.* (NA49 Collaboration), Phys. Rev. Lett. **82**, 2471 (1999); F. Siklér *et al.* (NA49 Collaboration), Nucl. Phys. A **661**, 45c (1999).
- [21] T. Matsui and H. Satz, Phys. Lett. B **178**, 416 (1986).
- [22] J.-Y. Ollitrault, Phys. Rev. D **46**, 229 (1992).
- [23] X.N. Wang and M. Gyulassy, Phys. Rev. Lett. **68**, 1480 (1992).
- [24] B. Zhang, C.M. Ko, and M. Gyulassy, Phys. Lett. B **455**, 45 (1999).
- [25] B. Zhang, C.M. Ko, B.A. Li, Z. Lin, and B.H. Sa, Phys. Rev. C **62**, 054905 (2000).